Expanded View Figures

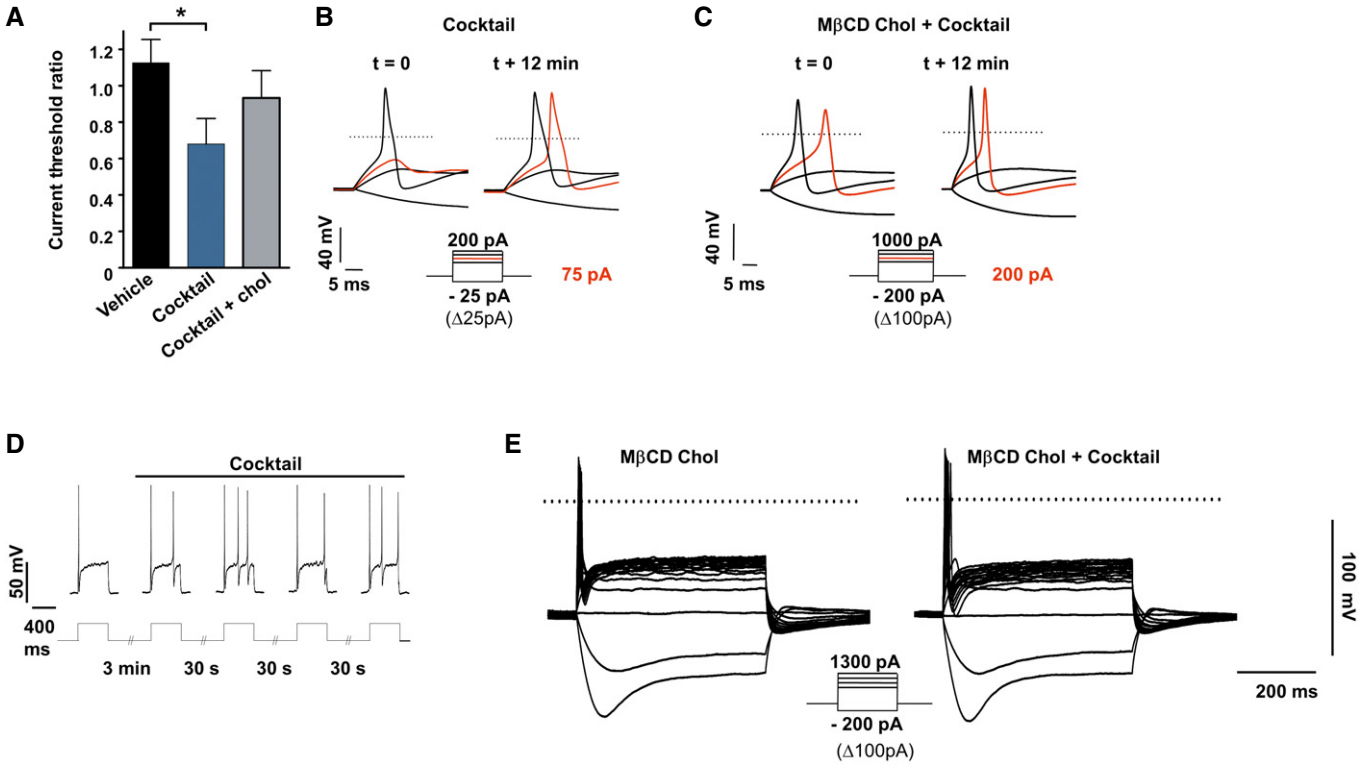

Figure EV1. Increased excitability induced by the inflammatory cocktail is prevented by soluble cholesterol.

A Ratio of current threshold for AP determined in DRG neurons treated with vehicle (n = 5) or with the inflammatory cocktail (1×) pre-treated (n = 5) or not (n = 7) with MβCD-chol (20 mM) for 10 min. For each cell, the current threshold was measured before (t = 0) and 12 min after bath application of the cocktail or its vehicle. Values are shown as mean ± standard error of the mean (SEM). Results were analyzed with a Mann–Whitney U-test. *$P < 0.05$.

B, C Representative recordings of current threshold for AP before (t = 0) and 12 min after bath application of the inflammatory cocktail in DRG neurons pre-treated (C) or not (B) with MβCD-chol. For clarity's sake, not all traces were illustrated. The red traces represent the voltage response induced by the injected current necessary to induce an action potential at t = 12 min. The dashed lines indicate 0 mV.

D Enhanced firing of a DRG neuron (27 pF) after bath application of the inflammatory cocktail. Injected current: 100 pA.

E Inhibition of inflammatory cocktail-induced hyperexcitability in a DRG neuron pre-treated with MβCD-chol (20 mM).

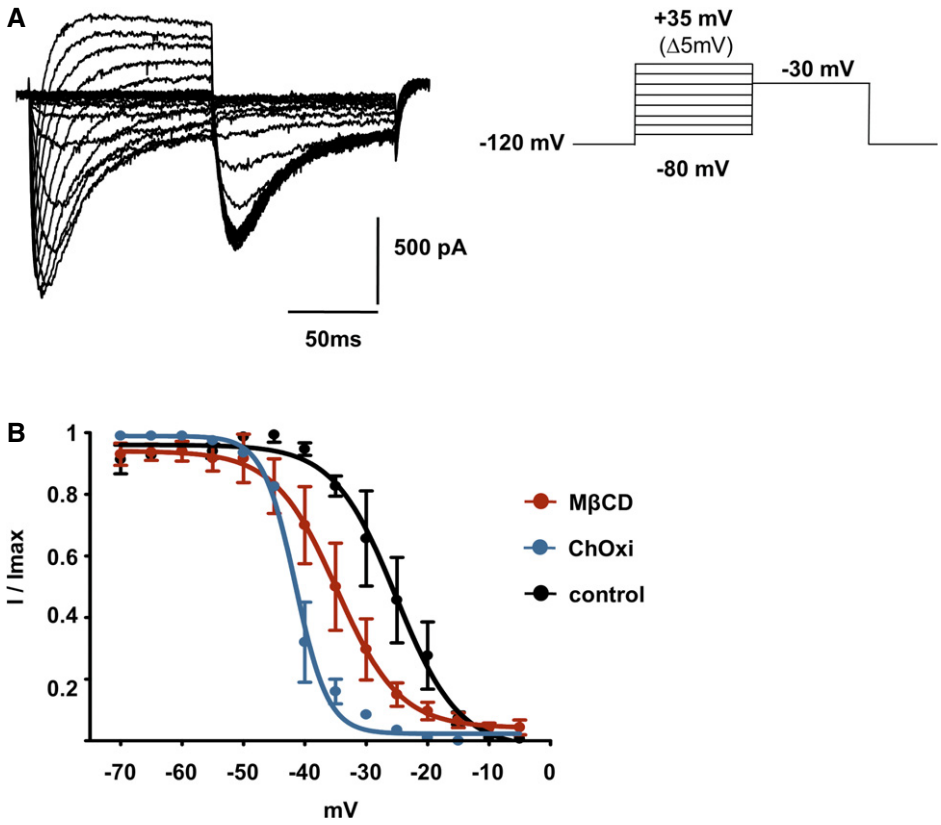

Figure EV2. Cholesterol depletion negatively shifts the "fast" inactivation voltage dependency of Nav1.9.

A Families of Nav1.9 current traces recorded after 10-min treatment with 20 mM MβCD. The test pulse to −30 mV was preceded by a family of depolarizing pulses ranging from −80 to 35 mV for 100 ms, while the cell was held at −120 mV.

B Fast inactivation curves of Nav1.9 current in control DRG neurons (n = 3) and in neurons treated with 20 mM MβCD (n = 3) or 2 U/ml ChOxi (n = 2) for 10 min. Curves were fitted by using single Boltzmann equations, yielding $V_{0.5}$ values of −25.17 ± 1.14, −34.8 ± 1.1, and −41.54 ± 0.38 mV, respectively. Values are shown as mean ± standard error of the mean (SEM).

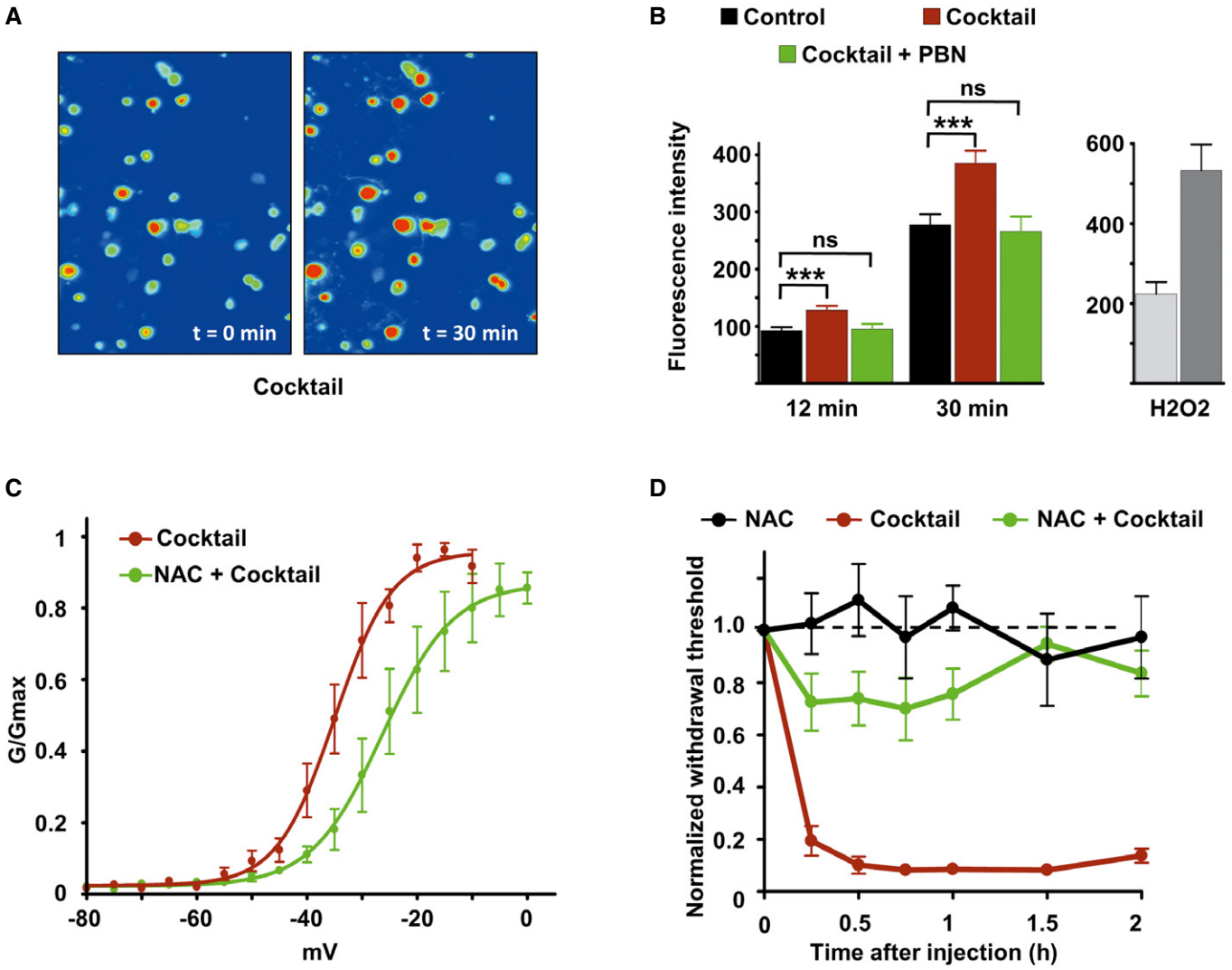

Figure EV3. The inflammatory cocktail causes pain hypersensitivity through production of increased reactive oxygen species.

A Imaging of DRG neurons loaded with the ROS-sensitive probe H_2DCFDA before (t = 0) and 30 min after inflammatory cocktail application.

B Left panel: Fluorescence intensity of cultured DRG neurons loaded with ROS-sensitive probe H_2DCFDA in control neurons (black bars, n = 114), neurons treated with the inflammatory cocktail (red bars, n = 119), and neurons co-treated with inflammatory cocktail and 4 mM of the ROS scavenger alpha-phenyl-N-tert-butyl nitrone (PBN, green bars, n = 95). Measure of fluorescence intensity was made 12 and 30 min after drug application. Right panel: positive control for ROS detection. DRG neurons (n = 15) were treated with 0.3% H_2O_2 and imaged at 12 (light gray) and 30 min (dark gray) after drug application. Fluorescence intensity (B) was analyzed with a non-parametric Mann-Whitney U-test. ***$P < 0.001$.

C Activation curves of Nav1.9 current fitted with single Boltzmann equations giving $V_{0.5}$ values of −35.02 ± 0.79 mV (n = 3, black line) and −26.34 ± 1.5 mV (n = 8, green line) for cells treated with the cocktail or with cocktail + NAC, respectively. Current were recorded 10 min after adding drugs.

D Comparison of mechanical hypersensitivity induced by intraplantar injection of NAC (n = 5, 20 mM), cocktail (20×, n = 4), and NAC + cocktail (n = 9). Note that the effects of cocktail were strongly reduced by NAC when injected simultaneously.

Data information: All values are shown as mean ± standard error of the mean (SEM).

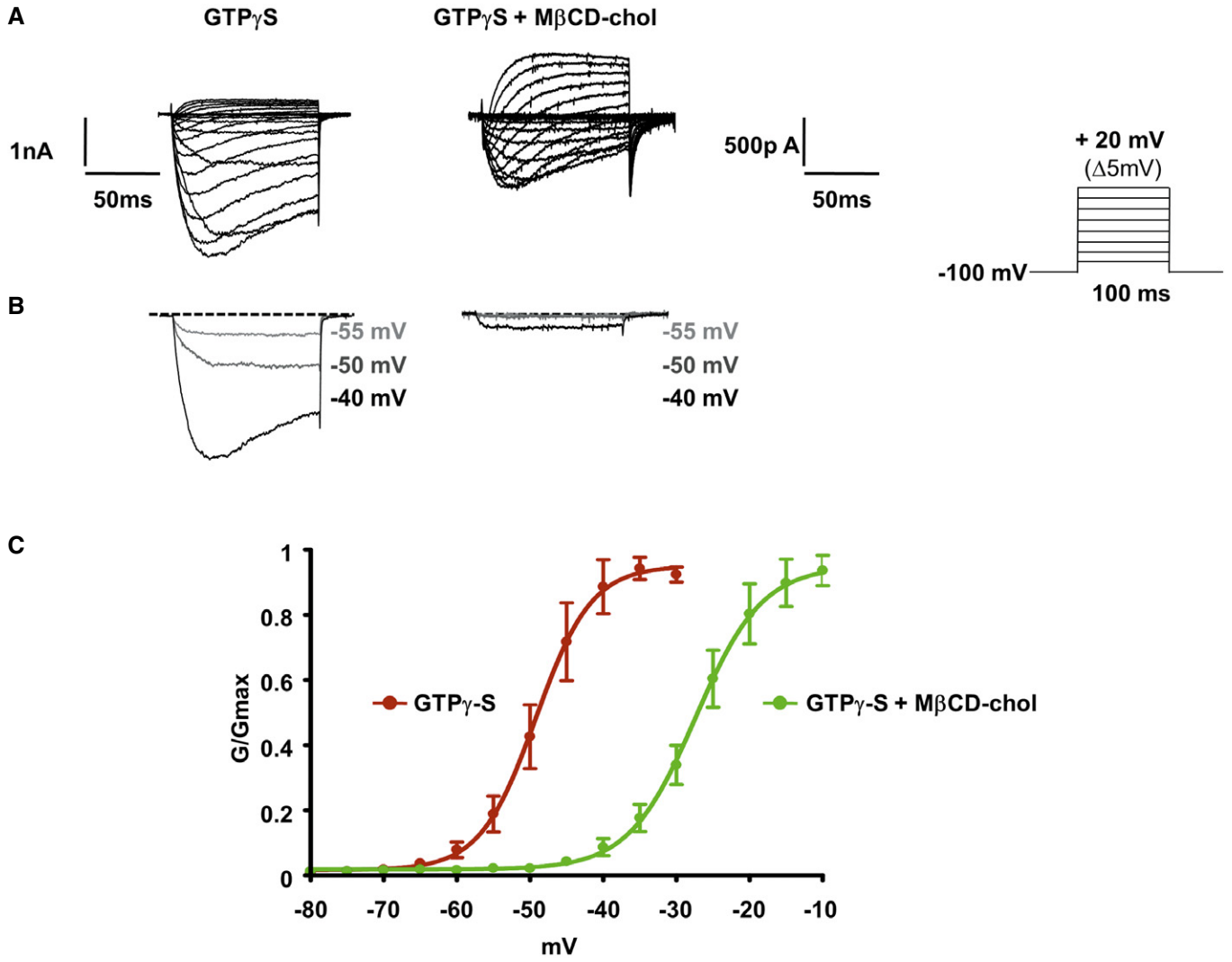

Figure EV4. Activation of Nav1.9 by GTPγS, a non-hydrolyzable G protein-activating analog of GTP, is prevented by soluble cholesterol.

A Representative current traces evoked by 100-ms depolarizing voltage steps from −80 to +20 mV (Δ5 mV, Vh = −100 mV). Nav1.9 currents were recorded 10 min after achieving whole-cell recording configuration with patch pipette solution containing 400 μM of GTPγS. In the right panel, DRG neurons were pre-incubated prior recording with MβCD-chol (20 mM) for 10 min.

B Currents evoked at −55, −50, and −40 mV from (A) are illustrated.

C Corresponding activation curves of Nav1.9 current fitted with a single Boltzmann equation. Values for $V_{0.5}$ of activation are −27.4 ± 0.7 mV (n = 7, green line) and −49.2 ± 0.8 mV (n = 8, red line) with and without MβCD-chol, respectively. Values are shown as mean ± standard error of the mean (SEM).

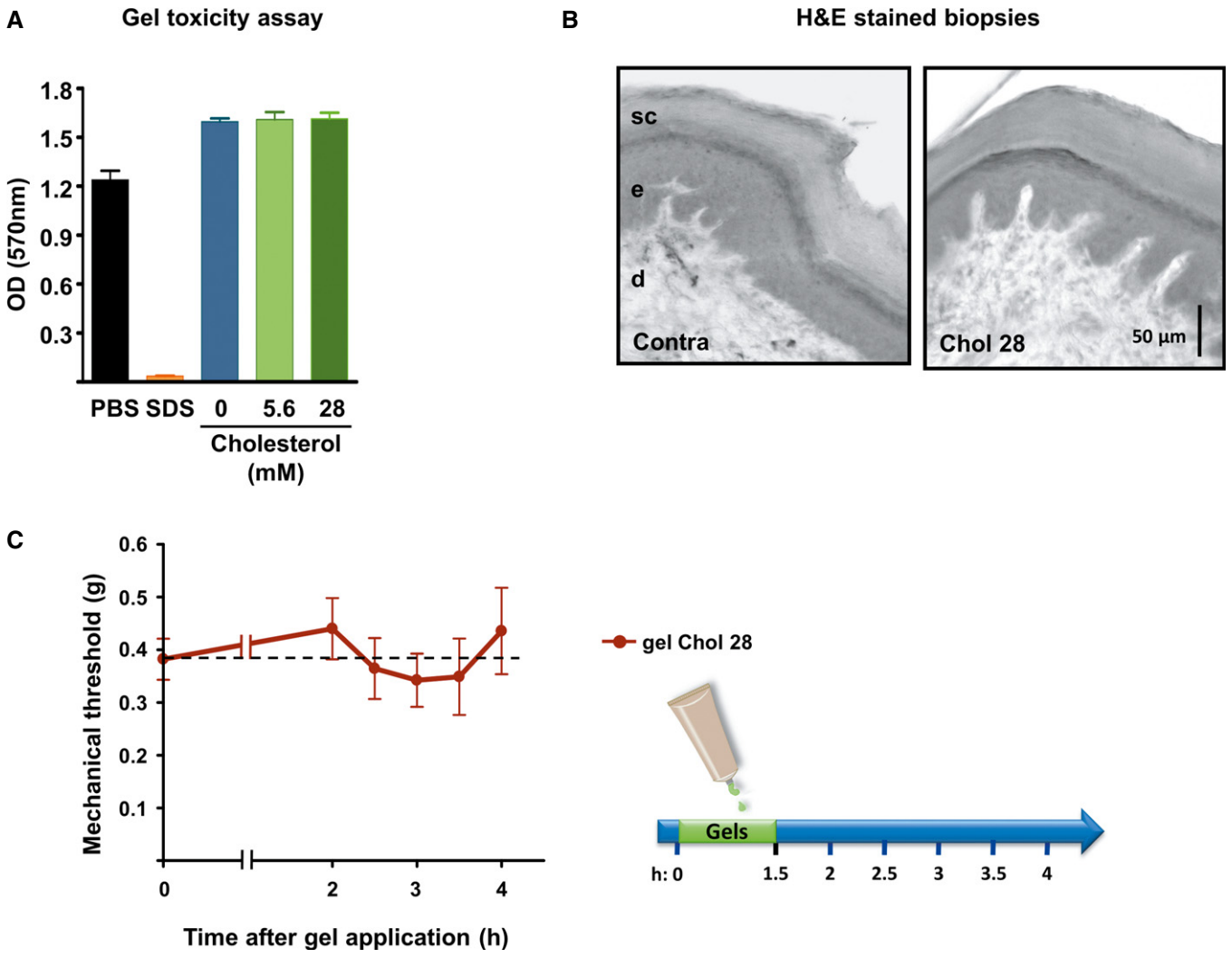

Figure EV5. Cholesterol gels do not impair cell viability, skin structure, and mechanical threshold.

A Cell viability of reconstructed human epidermis measured with an MTT assay 48 h after exposure to PBS (non-toxic control, n = 3), 5% SDS (toxic control, n = 3), HEC gel containing no cholesterol (0 mM, n = 3), and HEC gels containing soluble cholesterol at the concentration of 5.6 or 28 mM (n = 3 each).

B Hematoxylin–eosin staining of standardized skin biopsy specimen from paw treated for 1.5 h with an HEC gel containing 28 mM of cholesterol. sc: stratum corneum; e: epidermis; d: dermis.

C Mechanical withdrawal threshold of mice treated for 1.5 h with an HEC gel containing 28 mM of cholesterol (n = 9).

Data information: All values are shown as mean ± standard error of the mean (SEM).